Optimization Based Parameter Identification of the Caltech Ducted Fan [1]

Ryan Franz[2] John Hauser[3]

Abstract

Recent work [4] has demonstrated the use of model predictive control (MPC) for stabilizing the Caltech ducted fan. In results published up until now, however, additional stability augmentation was required. It was felt that an inadequate model was the cause of this shortcoming. This paper details an optimization-based parameter identification scheme which was used to identify new parameters for the ducted fan model. In addition to solving a traditional least squares optimization problem over the space of parameters, we introduce the additional concept of optimizing over the space of inputs as in a typical optimal control problem. The projection operator approach to trajectory optimization described in [5] is used to perform the trajectory optimization and enables many iterations to be executed in a reasonable time span. In the end, the newly identified parameters enabled us to use pure MPC with no additional stability augmentation. We were unable to achieve the same results consistently with other techniques. **Keywords:** System Identification, Nonlinear Systems, Parameter Identification, Parameter Optimization, Trajectory Optimization

1 Introduction

Methods for the identification of nonlinear systems can be broken into two distinct branches: model-based techniques and model-less, or black-box techniques. Model-based techniques assume some sort of *a priori* knowledge about the plant structure and dynamics, while black-box approaches are aimed at plants where little or nothing is known. This paper arises out of work on the Caltech Ducted Fan [9], which has dynamics conducive to analytical determination. Indeed, this is the case on most flight vehicles. For this reason a model-based approach is applicable.

The Caltech Ducted Fan is a testbed for control of unmanned aerial vehicles (UAVs), built to emulate aerodynamic flight in two dimensions in a safe and consistent environment. Over the past three years, a rigid-body aerodynamic model of the ducted fan has been used which captures the salient features of the dynamics (see section 4). This model contains many parameters, however, which are not easy to measure directly. These parameters have been identified many times using an equilibrium manifold approach (see [6] and section 4), but the uncertainties in the system revealed that other identification tools needed to be built to complement this method. These tools needed to be able to deal with more dynamic data, adapt parameters to fit possibly unmodeled dynamics, and in general validate parameters computed using the existing approach. We hope this can better provide us with a confirmation of our full model structure.

The goal of any model-based system identification procedure is straightforward: one attempts to select model parameter values in such a manner that the model response best matches the experimental response. The notion of "best" could vary greatly; following in the footsteps of Gauss, however, "best" in a least squares sense has been a natural choice. Indeed, this is precisely what we decided on for our new identification tool. The novelty of our approach, however, lies in the definition of model response. Given a choice of parameters ρ and a set of experimental data, we define the model response to be the trajectory $(x(\cdot), u(\cdot))$ of the system model $\dot{x} = f(x, u, \rho)$ closest to the given experimental data $(x_d(\cdot), u_d(\cdot))$. By closest, we mean closest in the L_2 sense, suggesting the solution to a standard optimal control problem.

We propose that this definition of model response provides some strong advantages:

- with proper cost weights in the definition of the model response, the effect of disturbances and certain unmodeled dynamics can be reduced on the overall optimization. This can be taken even to the point of introducing a disturbance input to the model which can be optimized over as well.
- the overall optimization does not depend as heavily on estimates of state variables which are not directly sensed; with proper cost weightings, the closest trajectory can be thought of as an optimal estimate of the actual full state.
- if the standard notion of model response is used, i.e. the closed loop response of the model at-

[1] Research supported in part by DARPA grant F33615-98-C-3613

[2] Northrop Grumman Space Technology, One Space Park Drive, Redondo Beach, CA

[3] Electrical and Computer Engineering, University of Colorado, Boulder, CO 80309-0425

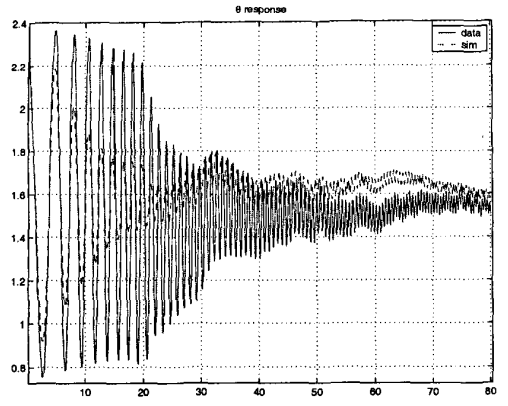

Figure 1: θ response while tracking a chirp data set

tempting to track the experimental data, then an appropriate feedback law must be used. This is not an obvious choice. With our approach this is computed as part of the optimization.

2 Motivation

When we first began to design an optimization-based identification tool which would attempt to match the model response, we performed the most obvious optimization:

$$\min_{\rho} \int_0^T \tfrac{1}{2}\|x(\tau) - x_d(\tau)\|_Q^2 + \tfrac{1}{2}\|u(\tau) - u_d(\tau)\|_R^2 \, d\tau + \tfrac{1}{2}\|x(T) - x_d(T)\|_P^2 \quad (1)$$

$$\text{s.t.} \quad \dot{x} = f(x, u, \rho), \quad u = K(x, t)$$

where the tracking control law $u = K(x,t)$ was necessary to stabilize the system, and needed to be designed to track the data in a reasonable fashion. This is not always an easy task, however—for example, figure 1 shows the response in θ (see section 4 below) when trying to track a certain data set using an LQR controller which seemed very reasonable. The response is very different, and could very well be far enough away that an optimization routine may not be able to find a meaningful answer.

Because of this, we sought an optimization which would not depend on designing a good control law; optimizing over the trajectory $(x(\cdot), u(\cdot))$ of the model as in a typical optimal control problem seemed a good choice.

3 Approach

Our identification problem can be stated as:

$$\min_{\rho} \min_{(x,u)} \int_0^T \tfrac{1}{2}\|x(\tau) - x_d(\tau)\|_Q^2 + \tfrac{1}{2}\|u(\tau) - u_d(\tau)\|_R^2 \, d\tau + \tfrac{1}{2}\|x(T) - x_d(T)\|_P^2 \quad (2)$$

$$\text{s.t.} \quad \dot{x} = f(x, u, \rho) \quad (3)$$

Our data is given by $(x_d(\cdot), u_d(\cdot))$, our model parameterized by ρ is given by equation (3), and weights Q and R define the cost. Let $x \in \mathbb{R}^n$, $u \in \mathbb{R}^m$ and $\rho \in \mathbb{R}^p$.

The overall optimization problem is solved as follows: the outer loop minimization over ρ is solved using a nonlinear least squares solver, where at every iteration the inner minimization over the trajectory $(x(\cdot), u(\cdot))$ must be solved for the current value of ρ by using the projection operator method [5].

3.1 Projection Operator Approach to Trajectory Optimization

The inner minimization problem is solved using the projection operator approach to trajectory optimization [5]. This approach provides accurate solutions to the optimization at hand in a reasonable amount of time. A brief explanation of the algorithm is given here.

Since f may be inherently unstable, we take a trajectory tracking approach. To this end, suppose that $\xi(t) = (\alpha(t), \mu(t))$, $t \geq 0$, is a bounded curve (e.g., an approximate trajectory of f) and let $\eta(t) = (x(t), u(t))$, $t \geq 0$, be the trajectory of f determined by the nonlinear feedback system

$$\begin{aligned} \dot{x}(t) &= f(x(t), u(t)), \qquad x(0) = \alpha(0), \\ u(t) &= \mu(t) + K(t)(\alpha(t) - x(t)) \, . \end{aligned} \quad (4)$$

Under certain conditions on f and K, this feedback system defines a continuous, nonlinear *projection operator*

$$\mathcal{P} : \xi = (\alpha, \mu) \mapsto \eta = (x, u) \, .$$

First note that, independent of K, if ξ is a trajectory of f, then ξ is a fixed point of $\mathcal{P}$, $\xi = \mathcal{P}(\xi)$. Using $\mathcal{T}$ to denote the trajectory manifold, we see that $\xi \in \mathcal{T}$ if and only if $\xi = \mathcal{P}(\xi)$.

With a suitable projection operator in hand, we may use $\xi = (\alpha, \mu)$ as a *redundant* representation of the trajectory $\eta = \mathcal{P}(\xi)$. This robust representation of η is ideally suited to numerical computations since the approximation errors introduced by discretization in time and quantization in space are kept small by the stabilizing effect of the feedback. In contrast, if f is unstable, it is easy to find multiple trajectories for which the initial condition and control trajectories are the same to machine precision. A suitable feedback gain K may be constructed by, for example, solving a finite horizon linear regulator problem [1] about the trajectory η.

The projection operator $\mathcal{P}$ provides a convenient parameterization of the trajectories in the neighborhood of a given trajectory. Indeed, the tangent space $T_\xi\mathcal{T}$ of bounded trajectories of the linearization of $\dot{x} = f(x,u)$ about $\xi \in \mathcal{T}$ can be used to parameterize *all* nearby trajectories [7]. That is, given $\xi \in \mathcal{T}$, there is an $\epsilon > 0$ such that, for each $\eta \in \mathcal{T}$ with $\|\eta - \xi\| < \epsilon$ there is a *unique* $\zeta \in T_\xi\mathcal{T}$ such that $\eta = \mathcal{P}(\xi + \zeta)$. Note also that $\zeta \mapsto D\mathcal{P}(\xi) \cdot \zeta$ is the bounded *linear* projection operator defined by linearizing (4) about ξ.

The following Newton method is used for the optimization:

Algorithm (projection operator Newton method)
given initial trajectory $\xi_0 \in \mathcal{T}$
for $i = 0, 1, 2, \ldots$
redesign feedback K if desired/needed
search direction:

$$\zeta_i = \arg \min_{\zeta \in T_{\xi_i}\mathcal{T}} Dg(\xi_i) \cdot \zeta + \tfrac{1}{2} D^2 g(\xi_i) \cdot (\zeta, \zeta) \quad (5)$$

step size $\gamma_i = \arg \min_{\gamma \in (0,1]} g(\xi_i + \gamma \zeta_i)$

update $\xi_{i+1} = \mathcal{P}(\xi_i + \gamma_i \zeta_i)$ (6)

end

Where $g(\xi)$ is the function to be minimized in equation (2). This algorithm is quite similar to the usual Newton method for unconstrained optimization of a function $g(\cdot)$ (e.g., in finite dimensions). As usual, the second order Taylor polynomial is used as a quadratic model function for determining a descent direction. A pure Newton method would, of course, use a fixed step size of $\gamma_i = 1$—the line search is common for expanding the region of convergence. The key differences are that 1) the search direction minimization (5) is performed on the tangent space to the trajectory manifold and 2) the update (6) *projects* each iterate on to the trajectory manifold. [5] shows the local quadratic convergence of this algorithm; the algorithm is stopped when either $Dg(\xi_i) \cdot \zeta$ (the search direction at the final time) falls below a certain threshold or the step size γ_i does not provide sufficient decrease.

3.2 Least Squares Minimization

Once the inner minimization in equation (2) has been solved for a given ρ, the optimal set $\xi_\rho^* = (x_\rho^*, u_\rho^*)$ is at a fixed point of the projection operator:

$$\xi_\rho^* = \mathcal{P}(\rho, \xi_\rho^*)$$

Accordingly, if we wish to minimize $h(\mathcal{P}(\rho, \xi_\rho^*))$ with respect to the parameters ρ, the gradients are given by:

$$D_\rho h(\mathcal{P}(\rho, \xi_\rho^*)) = Dh(\mathcal{P}(\rho, \xi_\rho^*)) D_\rho(\mathcal{P}(\rho, \xi_\rho^*))$$

In our case $h(\cdot)$ is the L_2 norm and the projection operator $\mathcal{P}$ is the state feedback defined in equation (4). $D_\rho(\mathcal{P}(\rho, \xi_\rho^*))$ is calculated by simulating the projection operator forward in time again and in addition solving:

$$\begin{aligned} D_\rho \dot{x} &= [D_x f + D_u f D_x u] D_\rho x + D_\rho f \\ D_\rho u &= -K D_\rho x \qquad D_\rho x(0) = 0 \end{aligned}$$

to provide us with the necessary gradients at each time step. In this paper we have used the Matlab function `lsqnonlin` [3] to carry out the least squares optimization using these gradients; we have also approximated the L_2 norm by

$$\sum_i \|x_\rho^*(t_i) - x_d(t_i)\|_Q + \|u_\rho^*(t_i) - u_d(t_i)\|_R \quad (7)$$

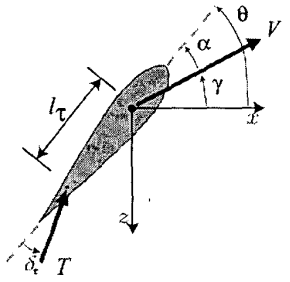

Figure 2: Ducted Fan Inertial Coordinate Frame

4 Caltech Ducted Fan Model

This analysis uses the inertial coordinate frame for the ducted fan, illustrated in fig. 2. This results in a sixth order model as shown below:

$$\ddot{x} = \frac{1}{m_x}\left[\cos\theta f_x + \sin\theta f_z + \frac{1}{2}\rho_d S V(\dot{x} C_L(\alpha) - \dot{z} C_D(\alpha))\right]$$

$$\ddot{z} = \frac{1}{m_z}\left[\cos\theta f_z - \sin\theta f_x - \frac{1}{2}\rho_d S V(\dot{x} C_L(\alpha) + \dot{z} C_D(\alpha)) + m_z g\right]$$

$$\ddot{\theta} = \frac{1}{I_{yy}}\left[l_\tau f_z + \frac{1}{2}\rho_d V^2 C_M(\alpha) S \bar{c} - b_\theta \dot{\theta}\right]$$

Where $S = 0.6\ m/s^2$ is the surface area, $\bar{c} = 0.5\ m$ is the mean chord, $\rho_d = 1.2\ kg/m^2$ is the air density, and $l_\tau = 0.35\ m$ is the moment arm from the center of mass to the point of application of the thrust T. V is the magnitude of the velocity given by

$$V = \sqrt{\dot{x}^2 + \dot{z}^2}$$

f_x and f_z are the x and y components of the thrust force T derived from inputs T and δp as

$$f_x = T\cos(\delta\tau) \quad (8)$$

$$f_z = -T\sin(\delta\tau) \quad (9)$$

$$\delta\tau = K_{\delta\tau}\delta p \quad (10)$$

Where $K_{\delta\tau} = 0.6228$ is the gain from the angle of the thrust vectoring bucket δp and the actual thrust angle $\delta\tau$. The relation between motor voltage input and thrust T is assumed to be

$$T = 38.89 V_m - 3.14 \quad (11)$$

The aerodynamic components for lift, drag and moment are modeled by:

$$\begin{aligned} C_L &= C_{L\alpha}(\alpha - \alpha_0) \\ C_D &= C_{D0} + \tfrac{1}{2} C_{D\alpha}(\alpha - \alpha_0)^2 \\ C_M &= C_{M\alpha}(\alpha - \alpha_0) \end{aligned} \quad (12)$$

Our final model, then, contains 6 states and 2 inputs as defined by:

$$x = \begin{bmatrix} x \\ \dot{x} \\ z \\ \dot{z} \\ \theta \\ \dot{\theta} \end{bmatrix} \quad u = \begin{bmatrix} V_m \\ \delta p \end{bmatrix} \quad (13)$$

Proceedings of the American Control Conference
Denver, Colorado June 4-6, 2003

The parameters we would like to identify are: m_x, the inertia in the x direction; m_z, the inertia in the z direction; g, the adjusted gravity; b_θ, the coefficient of friction in the θ direction; and the aerodynamic parameters α_0, $C_{L\alpha}$, C_{D0}, $C_{D\alpha}$ and $C_{M\alpha}$. These parameters were chosen because they cover all aspects of the model while remaining linearly independent.

4.1 Equilibrium Manifold Approach to Parameter Estimation

The model as stated above contains many parameters which must be identified. Some, such as m_z (z inertia) and g (gravity), can be measured with some degree of accuracy, but others, especially the aerodynamic coefficients, require looking at flight data to obtain an estimate. The approach taken with the aerodynamic coefficients $[C_L\ C_D\ C_M]$ has been to attempt to fly the ducted fan in level flight (either in closed loop or by hand) at several different velocities in order to obtain an equilibrium map of $(V\ \theta\ V_m\ \delta p)$. From this, curves of C_L, C_D and C_M can be calculated and then fit using any desired curve. Fig. 3 shows the equilibrium manifold relation between V and α, while fig. 4 shows the C_L curve. One advantage of this technique is that expressions for the coefficients need not be restricted to those shown in equation (12), which turn out to be very poor for high angles of attack.

While the above approach has proved to be very successful in the past, its static nature is a shortcoming. We needed a tool to understand the dynamic behavior of the ducted fan, where stiction is less influential and the effect of unmodeled dynamics is greater. As an example, at high velocities the aerodynamic effects of the thrust nozzle are very noticeable. Our hope was to lessen these effects by adjusting the existing model using optimization on dynamic data. As an additional benefit, we wanted to address certain other shortcomings of the equilibrium manifold approach. It is important to note, for example, that the calculation of the C_L and C_D curves assumes correct values of all other parameters, such as m_x, m_z and g. The next section details the application of the optimization based approach described above, which attempts to address these issues.

5 Application to Caltech Ducted Fan

In applying the identification algorithm to the ducted fan, we chose to decompose the problem. First, we used it on data taken in each of the three degrees of freedom separately while holding the other two fixed. This allowed us to isolate parameters which only acted in one axis, and to compute good approximations for parameters which acted in multiple axes. These approximations were then used as initial guesses for the full 3 DOF problem.

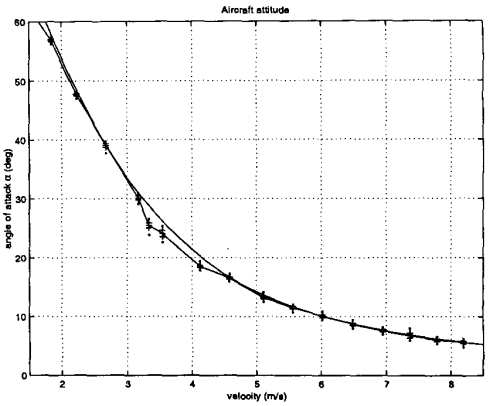

Figure 3: Experimentally Determined Equilibrium Manifold for the Ducted Fan

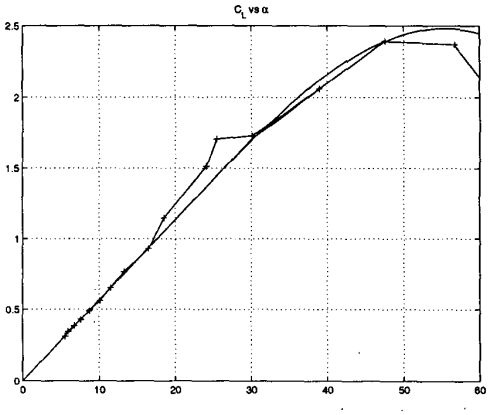

Figure 4: Lift and Drag Coefficient Curves Derived from the Equilibrium Manifold

5.1 x Direction Identification

With the z and θ directions fixed, we input a constant motor voltage V_m until the velocity $\dot{x}$ either reached a steady state or reached $12.5m/s$, at which point we set the input to 0. We performed this at three different values of V_m. The dynamics become:

$$\ddot{x} = \frac{1}{m_x}\left(-\frac{1}{2}\rho_d S C_{D0}\dot{x}^2 + T\right)$$

The parameter set used was $\rho = (m_x, C_{D0})$. In order to take into account the three different experiments with different values of V_m, we adopted a strategy of combining several segments from different data sets and optimizing over all of them. In this case, the projection operator optimization was applied to each segment separately at each iteration before returning the error to the least squares solver. In choosing which segments to use, we noted first that the deceleration portions of the data, with $T = 0$, were governed by dynamics

$$\ddot{x} = \frac{1}{m_x}\left(-\frac{1}{2}\rho_d S C_{D0}\dot{x}^2\right)$$

and thus the two elements being optimized affect the cost in the same way. Although the optimal input com-

puted may not have precisely $T = 0$, it will still be quite small. To avoid an optimization that was weighted more on this data, we cut each data set into two segments: the first segment being the full acceleration portion of length t_a seconds and the second segment being the following t_a seconds of the deceleration portion. In total, then, we used six segments of data.

5.2 z Direction Identification

With the x and θ directions fixed, we used a joystick control to control the motor voltage V_m and fly a roughly sinusoidal trajectory in z without exceeding the upper and lower limits. We used one segment of 180 seconds of this data to perform the optimization. The dynamics were taken to be:

$$\ddot{z} = \frac{1}{m_z}\left(\frac{1}{2}\rho_d S C_{D0}\dot{z}^2 \mathbf{sgn}(z) + m_z g - T\right)$$

The optimized parameters were $\rho = (m_z, g, C_{D0})$.

5.3 θ Direction Identification

With the x and z directions fixed, we used a simple PD controller to attempt to track a sinusoidal chirp signal with θ. This was performed several different times with different constant values of V_m, different orientations of the fan and different chirp parameters. The idea behind the different orientations was to find an optimal set of parameters with respect to all angles; for example, at $\theta = 90°$ there is a ground effect that changes the effect of the thrust. The dynamics are:

$$\ddot{\theta} = \frac{1}{I_{yy}}\left(-b_\theta - l_r T \sin(K_{\delta\tau}\delta p)\right)$$

The optimized parameters were: $\rho = (I_{yy}, b_\theta)$. Eight sets of data were used in the final optimization.

5.4 Full 3 DOF Identification

For the full 3 DOF identification, we used data taken while flying the fan in forward flight between 5 and 7 m/s with roughly sinusoidal maneuvering in z. An attempt was made to keep the angle of attack between $\pm 17°$, since the aerodynamic coefficients as defined in equation (12) are reasonable in this range. A single data set of 80 seconds was used for optimization. As mentioned in section 4, the parameter set used was: $\rho = (m_x, m_z, g, b_\theta, \alpha_0, C_{L\alpha}, C_{D0}, C_{D\alpha}, C_{M\alpha})$.

6 Results

6.1 Single Axis Identification

Table 1 shows the parameters obtained using the single axes data; for x and θ, the results using individual runs are shown as well as the results when they are combined. Initial guesses for the parameters were the values identified using either the equilibrium manifold method of section 4.1 or from static force measurements: $m_x = 8.5\ kg$, $m_z = 12.49\ kg$, $g = 0.599\ m/s^2$, $I_{yy} = 0.24\ kg\ m^2$, $b_\theta = 0.05$, $C_{D0} = 0.105$. The

axis	m_x	m_z	g	I_{yy}	b_θ	C_{D0}
static	**8.5**	**12.49**	**0.599**	**0.24**	**0.05**	**0.105**
x run1	7.021					0.098
x run2	7.909					0.099
x run3	7.780					0.102
x run4	8.340					0.099
x run5	8.664					0.094
x run6	8.334					0.099
x all	8.046					0.091
z		12.499	0.506			0.116
θ run1				0.137	0.094	
θ run2				0.145	0.085	
θ run3				0.135	0.090	
θ run4				0.144	0.072	
θ run5				0.132	0.099	
θ run6				0.131	0.094	
θ run7				0.118	0.075	
θ run8				0.131	0.075	
θ all				0.131	0.084	

Table 1: Results of Single Axis Identification

weights used for both the least squares optimization and the trajectory optimization were $Q = 2$, $R = 16$ and $P = 0$. In particular, the optimized value of the rotational inertia I_{yy} is much different than what we had identified in the past. Figure 5 shows response in θ for one small portion of data. The final results are much closer to the experimental data. The results for x and z are similar, but more difficult to see in a small plot. Figure 6 shows an example of the optimized input response for the z direction. It is difficult to see the difference between the optimal parameters curve and the real data, but the curve using the initial parameters is substantially different.

Runtimes for the computation of these solutions varied greatly, from a matter of minutes to upwards of one hour (on a slow laptop). The number of variables involved, however, especially for the x and θ directions, is very large. The data was taken with a sampling rate of $200Hz$, so the θ data at 800 seconds involved a vector of objective functions of length 160,000 for the least squares optimization.

6.2 Full 3 DOF Identification

The single axis results fixed the following values: $m_x = 8.046$, $m_z = 12.5$, $g = 0.5064$, $I_{yy} = 0.1305$, $b_\theta = 0.0843$, and $C_{M\alpha} = 0.0$. The full 3 DOF optimization provided the remaining values: $\alpha_0 = 0.0524\ rad$,$C_{L\alpha} = 3.93$,$C_{D0} = 0.105$,$C_{D\alpha} = 5.66$. Figure 7 shows the response in z for a representative portion of the data.

6.3 Use in MPC Model

The final parameters were used in a model predictive controller described in [4]. Previously, values from the equilibrium manifold identification method had been used, and we were unable to achieve full stabilization about hover without a PD controller to track desired

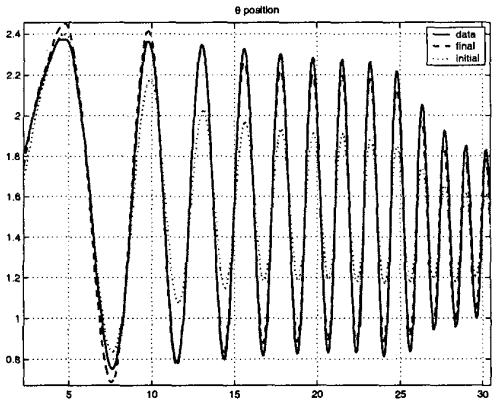

Figure 5: θ response to the initial and final parameters, as compared with data

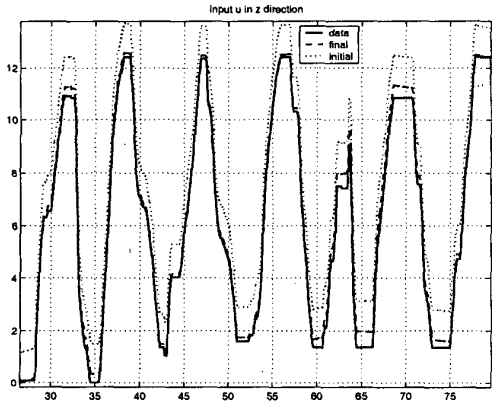

Figure 6: input for the z direction using the initial and final parameters, as compared with data

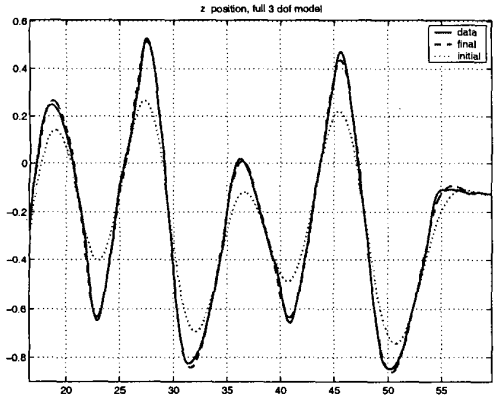

Figure 7: z response for the full 3 DOF model using the initial and final parameters, as compared with data

θ. With the new parameters, however, we were able to use pure MPC without this additional controller.

7 Conclusion

The approach we suggest in this paper would have been an intractable computational challenge a decade ago; the results in this paper, however, show the feasibility of the approach. The projection operator algorithm provides a good method for performing the trajectory optimization in a reasonable amount of time. The application of the approach to the Caltech Ducted Fan shows its practical merit, as parameters which can be difficult to ascertain by other methods are estimated in a full nonlinear sense. Furthermore, the parameters obtained enabled model-based controllers which were not possible before. Choices still remain, however, which must be made for effective use: which segments of data to use, and what costs will be best. We expect that with continued use of this identification tool we can set some guidelines as to how to make these choices.

References

[1] Brian D.O. Anderson and John B. Moore. *Optimal Control: Linear Quadratic Methods.* Prentice-Hall, 1990.

[2] Franky De Bruyne et al. Gradient expressions for a closed-loop identification scheme with a tailor-made parametrization. *Automatica*, 35:1867–1871, 1999.

[3] Thomas F. Coleman, Mary Ann Branch, and Andrew Grace. *Optimization Toolbox User's Guide.* The Math Works, Inc., Massachussetts, 1999.

[4] Ryan Franz, Mark Milam, and John Hauser. Applied receding horizon control of the caltech ducted fan. In *American Control Conference*, 2002.

[5] John Hauser. A projection operator approach to the optimization of trajectory functionals. In *15th IFAC World Congress*, 2002.

[6] John Hauser and Ali Jadbabaie. Aggressive maneuvering of a thrust vectored flying wing: A receding horizon approach. *Conference on Decision and Control*, 25:1–10, 2000.

[7] John Hauser and David G. Meyer. The trajectory manifold of a nonlinear control system. In *IEEE Conference on Decision and Control*, 1998.

[8] Tor A. Johansen. Identificatin of non-linear systems using empirical data and prior knowledge–an optimization approach. *Automatica*, 32:337–356, 1996.

[9] Mark Milam and R.M. Murray. A testbed for nonlinear flight control techniques: The caltech ducted fan. *Conference on Control Applications*, 25:1–10, 1999.